34th Annual International Conference of the IEEE EMBS
San Diego, California USA, 28 August - 1 September, 2012

3D Curve Constrained Deformable Registration Using a Neuro-Fuzzy Transformation Model

Xishi Huang, Anwar Bari, Sameer Zaheer, Thomas Looi, Jing Ren, and James Drake

Abstract— **Image registration of abdominal organs and soft tissues is considered daunting due to large organ shift and tissue deformation caused by patient motion, respiration, etc. In this study, we propose a novel neuro-fuzzy deformable registration technique that is constrained by 3D curves of vessel centerlines and point marks while minimizing strain energy. We present an analytical global optimal solution in the case when 3D curves, strain energy and point marks are considered, which will provide fast and robust deformable match for internal structures such as blood vessels, and significantly reduce the chance to get trapped in local minima. We have demonstrated the effectiveness of our deformable technique in registering liver MR images. Validation shows a target registration error of 1.98 mm and an average centerline distance error of 1.65 mm. This technique has the potential to significantly improve registration capability and the quality of intra-operative image guidance.**

I. Introduction

In this study, we investigate new techniques for deformable registration of soft tissues such as the liver. In order to guide therapeutic procedures and achieve more accurate diagnosis of diseases, it is often helpful to fuse together multiple liver images from different sources. Although image registration for mostly rigid structures such as the brain and bone is normally a manageable task, it is more difficult to align liver images where we have to deal with large organ shift and soft tissue deformation caused by patient motion, respiration, heartbeats, surgical manipulation, etc. There are similar challenges for other abdominal organs [1,2,3].

Blood vessels are critical structures of many organs and provide fundamental information in many clinical applications. Blood vessels are often imaging targets in different imaging modalities such as MRA, CTA and ultrasound, provide good features for image registration, and are good references for localizing targets deep inside organs. Vessels in the liver are dominant image features, which make them an ideal feature reference for image registration. However, it is still very challenging how to effectively use vessels in image registration since these vessel structures often cause intensity-based image registration algorithms to get trapped in local minima. In this study, we propose a novel neuro-fuzzy deformable registration technique that is constrained by 3D curves and point marks while minimizing strain energy caused by deformation of soft tissues. We present an optimal analytical solution in the case when 3D curves, strain energy and point marks are considered, which provides fast and robust deformable match for internal structures such as blood vessels, and significantly reduces the chance of getting trapped in local minima in image registration.

Our novel neuro-fuzzy transformation model consists of multiple region-based sub-models. The advantage is that each region can have a different model, which can be chosen according to deformation characteristics of regions. The strain energy constraint provides good generalization properties, prevents the issue of overfitting (for example, physically impossible deformation), and leads to physically consistent deformable match results. Sample sets of liver MR images of human subjects were used to evaluate the performance of the proposed registration approach.

II. Methods and Materials

A. Physics-Based Registration Methodology

In this study, we apply multiple techniques to address the challenge of nonlinear registration of images with soft tissue deformation. Our registration methodology is based on elastic solid mechanics and the minimum strain energy principle. We aim to minimize the following energy function consisting of four terms:

$$J = w_{im} E_{im}(x) + w_e E_e(x) + w_c E_c(x) + w_m E_m(x) \quad (1)$$

This energy function measures the quality of alignment between the fixed image and the transformed moving image. The first energy term $E_{im}(x)$ is image intensity-based normalized cross correlation (NCC). $E_e(x)$ is the strain energy produced by deformation of soft tissues. Minimization of strain energy will yield physically consistent/plausible deformation. The third energy term $E_c(x)$ is to minimize the distance between pairs of 3D curves (blood vessel centerlines) extracted from the fixed and moving images, which ensures that the resulting optimal deformation should align internal vessel structures. The last term $E_m(x)$ is the distance between corresponding point marks such as bifurcation points. Weights w_i are used to adjust relative effects of each term. Therefore, combination of the above four energy terms provides different mechanisms to constrain final registration solution to a

* Research supported by Canada Foundation for Innovation, Federal Economic Development Agency for Southern Ontario (SODA), and Ontario Research Foundation.

X. Huang is with the Department of Medical Imaging, University of Toronto and CIGITI, Hospital for Sick Children, 555 University Ave., Toronto, M5G 1X8, Canada (phone: 416-813-7654 x 28140; fax: 416-813-7477; e-mail: Edward.Huang@ sickkids.ca).

A. Bari and J. Ren is with the Faculty of Engineering and Applied Science, Univ. of Ontario Institute of Technology, Oshawa, ON, Canada

S. Zaheer, T. Looi, and J. Drake are with CIGITI, Hospital for Sick Children, 555 University Ave., Toronto, M5G 1X8, Canada.

physically consistent deformable match. Furthermore, if considering the last three energy terms, we provide a fast and robust analytical solution through specific design of different registration components.

B. Region-Based Neuro-Fuzzy Transformation Model

In this section, we propose a novel neuro-fuzzy transformation model that consists of N_R region-based sub-models. The advantage is that each region can have a different model, which can be chosen according to deformation characteristics of the region. In many cases, different deformation patterns occur only in local regions. Many local deformation models such as B-Spline and free-form deformation have been developed [4,5]. However, they generally require a large number of transformation parameters, which leads to large search space, making registration computationally intensive.

Neuro-fuzzy technique is a branch of artificial intelligence, which integrates artificial neural networks and fuzzy logic theory to take full advantage of both techniques. The main benefit of this approach is its learning and adaptation ability, good interpretability and easy integration of expert knowledge, that is, by using the fuzzy rules, the approach tries to simulate a person's line of thought in decision-making. We adopt adaptive neuro-fuzzy inference system (ANFIS) [6] to integrate region-based sub-models into a unified transformation model. Our neuro-fuzzy system has the following N_R rules:

Fuzzy rule *i*: If point *x* is in region R_i, then $x' = T_i(x)$

where *x* is a 3D point in the fixed image space, *x'* the corresponding transformed point, $T_i(x)$ a local transformation model specifically tailored to Region *i*. In summary, the overall transformation *T(x)* can be derived as [7],

$$x' = T(x) = \frac{\sum_{i=1}^{N_R} M_i(x) T_i(x)}{\sum_{i=1}^{N_R} M_i(x)} = \sum_{i=1}^{N_R} M_{ni}(x) T_i(x) \qquad (2)$$

$$M_{ni}(x) = M_i(x) \Big/ \sum_{i=1}^{N_R} M_i(x)$$

where $M_i(x)$ is the membership function of a fuzzy set associated with each region R_i.

By selecting an appropriate membership function for each region, transition of the transformation model from one region to another can be gradual or sharp, which provides great flexibility to achieve desirable transitions between the sub-models. Furthermore, with the help of flexibility to select an appropriate membership function associated with each region, we can easily choose proper local membership function to limit the effective range of a global transformation model to the desired region in our neuro-fuzzy model. Therefore, we can take full advantage of good generalization of global models and representation capability of local deformation of local models. To represent complex deformation in one region, we have the flexibility to either select a more complicated model or place more dense local models. All the local models are not necessarily distributed uniformly, so our model can reduce the total number of transformation parameters.

In this study, membership functions are selected as 3D Gaussian functions.

$$M_i(x) = \exp\left\{-\left[\frac{(x-c_{ix})^2}{2\sigma_x^2} + \frac{(y-c_{iy})^2}{2\sigma_y^2} + \frac{(z-c_{iz})^2}{2\sigma_z^2}\right]\right\} \qquad (3)$$

where (c_{ix}, c_{iy}, c_{iz}) is the center of Region *i*, and parameters $(\sigma_{ix}, \sigma_{iy}, \sigma_{iz})$ are used to control the effective range of local model $T_i(x)$.

In general, the overall transformation model *T(x)* is nonlinear with respect to spatial position *x* and transformation parameters. However, if local models $T_i(x)$ are linear with respect to transformation parameters, transformation *T(x)* is also linear with respect to transformation parameters after membership functions are determined.

In this study, we choose linear transformation for each region, i.e. $T_i(x) = A_i x + b_i$. We can rewrite the overall transformation (2) for the whole image in the following form:

$$T(x) = A_p^T(x)\, p \qquad (4)$$

where $p \equiv [\,p_{T1}^T \quad p_{T2}^T \quad \cdots \quad p_{TN_R}^T\,]^T$ is the total transformation parameters of $T(x)$, p_{Ti} is the corresponding 12 parameters (A_i, b_i) of $T_i(x)$.

Note that transformation *T(x)* is linear with respect to parameters *p*. Combined with 3D curves, point marks and strain energy, this linearity leads to fast analytical solution when these three energy terms are taken into account.

C. 3D Curve Representation Using B-Spline

The centerlines of blood vessels are extracted from MR liver images in the form of discrete points. In order to effectively employ these 3D curves as constraints in image registration, we need a continuous and smooth representation. In this study, we express vessel centerlines as parametric 3D curves using the 2nd order B-Spline. This representation leads to an analytical solution to the closest point on the curve given a transformed point of fixed curves. Note that we only need a continuous representation for centerlines in the moving image, but not for those in the fixed image.

The *i*-th vessel centerline in the moving image $C_{mi}(t)$ is represented as three 1D parametric B-Spline curves.

$$C_{mi}(t) = \left[C_{mix}(t) \quad C_{miy}(t) \quad C_{miz}(t)\right]^T,\ t \in [t_k, t_{k+1}],$$
$$k = 0,1,\cdots, N_{mi} - 1$$
$$C_{mix}(t) = C_{mixk\,2}t^2 + C_{mixk\,1}t + C_{mixk\,0}$$
$$C_{miy}(t) = C_{miyk\,2}t^2 + C_{miyk\,1}t + C_{miyk\,0} \qquad (5)$$
$$C_{miz}(t) = C_{mizk\,2}t^2 + C_{mizk\,1}t + C_{mizk\,0}$$

where t is the parameter, can be selected to represent the curve length between current coordinates $C_{mi}(t)$ and the vessel starting point, N_{mi} is the number of discrete points on the i-th vessel centerline extracted from MR images, $(C_{mi*k2}, C_{mi*k1}, C_{mi*k0})$ are constants for the i-th curve.

D. Minimization of 3D Curve Energy

In this section, we propose a novel technique to analytically calculate the closest point on a 3D curve to a given point, and the derivative of the shortest distance between pairs of curves with respect to transformation parameters through a parametric representation of 3D curves.

Vessel centerlines can provide reliable constraints during the image match process. To make use of vessel centerlines, we aim to minimize the distance between pairs of corresponding vessel centerlines, which is formulated as the following optimization problem:

$$E_c(p) = \sum_{i=1}^{N_C} \sum_{k=1}^{N_{Ci}} \frac{1}{2} \left\| T(X_{fik}) - C_{mi}(t) \right\|^2 \tag{6}$$

where N_C is the total number of vessel centerlines, N_{Ci} the number of discrete points on the ith centerline from the fixed image, $X_{fik}, i = 1,2,\cdots,N_C, k = 1,2,\cdots,N_{Ci}$ is the k-th point on the i-th centerline from the fixed image, $C_{mi}(t)$ the continuous parametric representation of the i-th vessel centerline from the moving image. For simplicity we limit our discussion to finding the closest point on a 3D curve in the moving image for a transformed point of the fixed image.

$$\begin{aligned} E_{cik}(p) &= \frac{1}{2} \left\| T(X_{fik}) - C_{mi}(t) \right\|^2 = \frac{1}{2} \left\| X_{Tfik} - C_{mi}(t) \right\|^2 \\ &= \frac{1}{2} \left(X_{Tfik} - C_{mi}(t) \right)^T \left(X_{Tfik} - C_{mi}(t) \right), \quad X_{Tfik} = T(X_{fik}) \end{aligned} \tag{7}$$

From (5), we can rewrite the above $E_{cik}(p)$ in the form:

$$E_{cik} = \left(b_4 t^4 + b_3 t^3 + b_2 t^2 + b_1 t + b_0 \right). \tag{8}$$

Given the parameters (p_c) of current transformation $T(x)$ and X_{fik} on the fixed centerline, we first compute $X_{Tfik} = T(X_{fik})$. Next, we find the closest point $X_{cmik} = C_{mi}(t_{cmik})$ on vessel curve $C_{mi}(t)$ such that the corresponding optimal parameter

$$t_{cmik} = arc \min_t E_{cik} = \frac{1}{2} \left\| X_{Tfik} - C_{mi}(t) \right\|^2. \tag{9}$$

The optimal solution t_{cmik} is obtained by analytically solving the following cubic polynomial equation: $\frac{dE_{cik}}{dt} = f_d(X_{Tfik}, t) = a_3 t^3 + a_2 t^2 + a_1 t + a_0 = 0$ given X_{Tfik}. As we know, there exists an analytical formula to calculate the roots of cubic polynomials. If we choose a parametric representation of 3D curves with cubic B-Spline, we need to solve a 5-th order polynomial equation $\frac{dE_{cik}}{dt} = 0$. Unfortunately, no analytical solution exists in this case. This is the reason why we select the 2nd order of B-Spline to represent vessel centerlines so that we achieve a good balance between smooth curves and efficiency.

Because t_{cmik} is a function of X_{Tfik} and

$$\frac{df_d(X_{Tfik}, t)}{dX_{Tfikj}} = \frac{\partial f_d}{\partial X_{Tfikj}} + \frac{\partial f_d}{\partial t} \cdot \frac{\partial t}{\partial X_{Tfikj}} = 0 \tag{10}$$

the corresponding partial derivatives of t with respect to transformed discrete points X_{Tfik} are calculated as follows.

$$\frac{\partial t_{cmik}}{\partial X_{Tfik}} = -\frac{\partial f_d}{\partial X_{Tfik}} \Big/ \frac{\partial f_d}{\partial t}. \tag{11}$$

Now we derive an analytical formula to compute the derivative of $E_c(p)$ with respect to transformation parameters p.

$$\begin{aligned} &\frac{\partial X_{cmik}}{\partial p} = \frac{\partial C_{mi}(t)}{\partial p} = \left(\frac{\partial C_{mi}(t)}{\partial t} \right) \left(\frac{\partial t}{\partial X_{Tfik}} \right)^T \frac{\partial T}{\partial p}, \quad \frac{\partial T}{\partial p} = A_p^T(x) \\ &\frac{\partial E_{cik}}{\partial p} = \left(\frac{\partial X_{Tfik}}{\partial p} - \frac{\partial X_{cmik}}{\partial p} \right)^T \left(X_{Tfik} - X_{cmik}(t_{cmik}) \right) \\ &\quad = \left(\frac{\partial T}{\partial p} \right)^T \left(I_{3x3} - \left(\frac{\partial t}{\partial X_{Tfik}} \right) \left(\frac{\partial C_{mi}(t)}{\partial t} \right)^T \right) \left(X_{Tfik} - X_{cmik}(t_{cmik}) \right) \\ &\frac{\partial E_c(p)}{\partial p} = \sum_{i=1}^{N_C} \sum_{k=1}^{N_{Ci}} \frac{\partial E_{cik}}{\partial p} = \sum_{i=1}^{N_C} \sum_{k=1}^{N_{Ci}} \left\{ \left(\frac{\partial T}{\partial p} \right)^T \left(I_{3x3} - \left(\frac{\partial t}{\partial X_{Tfik}} \right) \left(\frac{\partial C_{mi}(t)}{\partial t} \right)^T \right) \left(X_{Tfik} - X_{cmik}(t_{cmik}) \right) \right\} \\ &\quad = \sum_{i=1}^{N_C} \sum_{k=1}^{N_{Ci}} \left\{ A_p(X_{Tfik}) D_{cmik}^T A_p^T(X_{Tfik}) \right\} p - \sum_{i=1}^{N_C} \sum_{k=1}^{N_{Ci}} \left\{ A_p(X_{Tfik}) D_{cmik}^T X_{cmik} \right\} \end{aligned} \tag{12}$$

Note that $\frac{\partial E_c(p)}{\partial p}$ is a linear function of parameters p, which implies that the shortest distance between curves $E_c(p)$ is a quadratic function of transformation parameters p.

E. Minimum Strain Energy

The strain energy term prevents the issue of overfitting, and leads to physically consistent deformable match results. The strain energy $E_{e(x)}$ is generated by deformation of soft tissues based on elastic solid mechanics, and can be calculated using the Saint-Venant model [8] as follows:

$$E_e = \iiint_\Omega W(E)\, dxdydz, \tag{13}$$

$$W(E) = 0.5\lambda \left(tr(E) \right)^2 + \mu \cdot tr(E^2), tr(E) \equiv e_{11} + e_{22} + e_{33}$$

where $W(E)$ is the strain energy density, E is a strain tensor, $E = \left(e_{ij} \right)_{3x3}$, $e_{ij} \approx \frac{1}{2} \left(\frac{\partial T_i}{\partial x_j} + \frac{\partial T_j}{\partial x_i} - 2\delta_{ij} \right)$, $\delta_{ij} = \begin{cases} 1, & if \ i = j \\ 0, & otherwise \end{cases}$.

From (4), we can write strain energy density as a quadratic function of the parameters p of our proposed neuro-fuzzy transformation model in the following formula:

$$W(E) = C_0(x) + C_1^T(x) p + p^T C_2(x) p \tag{14}$$

Therefore, we obtain a quadratic form of strain energy:

$$E_e(p) = C_{e0} + C_{e1}^T p + p^T C_{e2} p \tag{15}$$

$$C_{e0} = \iiint_\Omega C_0(x)\, dxdydz, \ C_{e1} = \iiint_\Omega C_1(x)\, dxdydz,$$

$$C_{e2} = \iiint_\Omega C_2(x)\, dxdydz$$

where constants (C_{e0}, C_{e1}, C_{e2}) can be calculated offline in advance based on the pre-operative image.

The explicit derivative of strain energy with respect to transformation parameters p is calculated as follows.

$$\frac{\partial E_e(p)}{\partial p} = C_{e1} + 2C_{e2}p \ . \tag{16}$$

F. Point Marks

Point marks are employed to anchor the deformation at some specific locations. Point marks such as bifurcations provide the most robust and efficient way to obtain correct registration. We assume that there are N_m pairs of corresponding point marks (i.e. bifurcation points), $(X_{fk}, X_{mk}), k = 1,2,\cdots,N_m$. Then we minimize the distance between corresponding point marks by adding the following term to the registration energy function,

$$E_m(p) = \sum_{i=1}^{N_m} \frac{1}{2} \left\| T(X_{fk}) - X_{mk} \right\|^2 \tag{17}$$

Its derivative with respect to transformation parameters can be analytically calculated through the following formula,

$$\frac{\partial E_m(p)}{\partial p} = \sum_{i=1}^{N_m} A_p(X_{fk}) \left(T(X_{fk}) - X_{mk} \right). \tag{18}$$

G. Analytical Optimal Solution Subject to Constraints of 3D Curves, Marks and Strain Energy

To obtain the optimal solution, 3D curves, point marks, and strain energy are employed to register the two images, and we set $w_{im} = 0$ in (1). The other three terms are quadratic functions of transformation parameters p. Therefore, the global optimal transformation parameters can be calculated analytically by solving linear equations $\partial J / \partial p = 0$.

This fast analytical solution can be used to dynamically update guidance vessel models for vessel extraction. It is expected to greatly improve the quality of vessel segmentation under the guidance of pre-operative vessel models in a joint registration and segmentation framework. This fast solution can be employed to initialize intensity-based image registration to the neighborhood of correct match. We expect that it would significantly reduce the probability of getting trapped in local minima.

III. Registration Results

All of the images used in this study were acquired from human volunteers. High-quality dynamic MR images were acquired in the axial plane using a 1.5T GE scanner (GE Medical Systems, Milwaukee, WI). Image acquisition was performed using the LAVA gradient echo sequence with TR=3.79 ms, TE=1.72ms, a flip angle of 12 degrees, an image matrix size of 256 x 256, in-plane pixel size of 1.3 mm x 1.3 mm and slice thickness of 1.5 mm. Image sets were acquired with a breath-hold at different positions.

The selected overlays of the centerlines after registration are shown in Fig. 1 using 10 sub-models, which demonstrate that the centerlines are matched well after registration. To quantitatively evaluate the registration accuracy, we calculated two accuracy metrics: target registration error (TRE) and average centerline distance (ACD). The resulting average TRE of 56 bifurcation points was 1.98 mm, and the average ACD of 111 vessel branches is 1.65 mm. These registration accuracy measures have demonstrated that the proposed deformable registration technique is able to accurately register two sets of images.

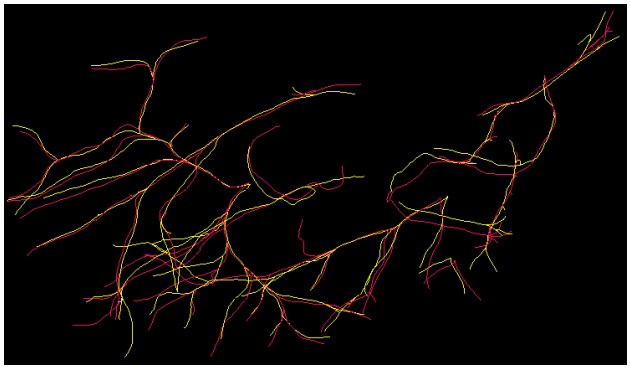

Figure 1. Overlay of centerlines after match. Red lines: left lateral decubitus, yellow lines: supine mapped to left lateral decubitus.

IV. Conclusion

We have presented a new approach to the registration of deformable liver images, which significantly reduces the number of transformation parameters in the proposed neuro-fuzzy model, and a fast analytical global optimal solution when considering 3D curves, point marks and minimum strain energy. Since the speed of registration is approximately proportional to the number of parameters, the proposed method has the potential to dramatically accelerate intra-operative image registration, making intra-operative image guidance possible in many abdominal and thoracic procedures.

Future work includes automatic extraction and match of vessel centerlines under joint extraction and registration framework, and more validation on clinical data and different MR contrasts.

References

[1] D.L. Hill, et al., "Medical image registration," Phys. Med. Biol., 46(3), pp. R1–45, 2001.

[2] K. Murphy, et al., "Evaluation of registration methods on thoracic CT: the EMPIRE10 challenge," IEEE Trans Med Imaging 30, pp. 1901-1920, 2011.

[3] M. Baumhauer, et al., "Navigation in endoscopic soft tissue surgery: perspectives and limitations," J. Endourol. 22(4), pp. 751-766, 2008.

[4] M. Holden, "A review of geometric transformations for nonrigid body registration," IEEE Trans Med Imaging 27(1), pp. 111-28, 2008.

[5] Rueckert, D. et al., "nonrigid registration using free-form deformations: application to breast MR images," IEEE Trans Med Imaging 18(8), pp. 712-721, 1999.

[6] R.J.S. Jang, "ANFIS: adaptive-network-based fuzzy inference system," IEEE Trans Syst Man Cybern 23, pp. 665-685, 1993.

[7] X. Huang, et al., "A soft computing framework for software effort estimation," Soft Computing 10, pp. 170-177, 2006.

[8] P.G. Ciarlet, *Mathematical Elasticity*, vol. 1, North Holland, 1988.